NeuroImage 52 (2010) 1149–1161

Contents lists available at ScienceDirect

NeuroImage

journal homepage: www.elsevier.com/locate/ynimg

Comments and Controversies

Spontaneous brain activity and EEG microstates. A novel EEG/fMRI analysis approach to explore resting-state networks

F. Musso [a,*,1], J. Brinkmeyer [a,b,*,1], A. Mobascher [c], T. Warbrick [a,b], G. Winterer [a,b]

[a] Neuropsychiatric Research Laboratory, Department of Psychiatry, Heinrich-Heine University Duesseldorf, Bergische Landstrasse 2, 40629 Duesseldorf, Germany
[b] Institute of Neurosciences and Biophysics, Helmholtz Research Center Juelich, Wilhelm-Johnen-Straße, 52428 Jülich Germany
[c] Dept. of Psychiatry Johannes Gutenberg-University Untere Zahlbacher Str. 8 55131 Mainz, Germany

ARTICLE INFO

Article history:
Received 9 October 2009
Revised 8 January 2010
Accepted 26 January 2010
Available online 6 February 2010

Keywords:
Resting-state networks
RSNs
BOLD
Hemodynamic response function
HRF
Functional magnetic resonance imaging
Electroencephalography
EEG segmentation
EEG microstates

ABSTRACT

The brain is active even in the absence of explicit input or output as demonstrated from electrophysiological as well as imaging studies. Using a combined approach we measured spontaneous fluctuations in the blood oxygen level dependent (BOLD) signal along with electroencephalography (EEG) in eleven healthy subjects during relaxed wakefulness (eyes closed). In contrast to other studies which used the EEG frequency information to guide the functional MRI (fMRI) analysis, we opted for transient EEG events, which identify and quantify brain electric *microstates* as time epochs with quasi-stable field topography. We then used this microstate information as regressors for the BOLD fluctuations. Single trial EEGs were segmented with a specific module of the LORETA (low resolution electromagnetic tomography) software package in which microstates are represented as normalized vectors constituted by scalp electric potentials, i.e., the related 3-dimensional distribution of cortical current density in the brain. Using the occurrence and the duration of each microstate, we modeled the hemodynamic response function (HRF) which revealed BOLD activation in all subjects. The BOLD activation patterns resembled well known resting-state networks (RSNs) such as the default mode network. Furthermore we "cross validated" the data performing a *BOLD independent component analysis* (ICA) and computing the correlation between each *ICs* and the EEG microstates across all subjects. This study shows for the first time that the information contained within EEG microstates on a millisecond timescale is able to elicit BOLD activation patterns consistent with well known RSNs, opening new avenues for multimodal imaging data processing.

Introduction

In almost two decades of functional magnetic resonance imaging (fMRI) studies the dominant method to obtain information on brain function has been measuring changes of brain activity in response to a task. At present, however, we are experiencing a "turn of the tide" in our analytical approach; a new avenue of neuroimaging research on *spontaneous fluctuations* of brain activity is emerging. These spontaneous fluctuations can be defined as "changes in brain activity not externally induced or voluntarily generated by the subject which occur during relaxed wakefulness" (Raichle and Snyder, 2007; Laufs, 2008). As highlighted by Fox and Raichle (2007) in their comprehensive review, there are good reasons to explore the resting fluctuation of brain activity. This is because the brain at rest is responsible for most of the ongoing cerebral energy consumption and task related increases in neuronal metabolism are usually less than 5% (Raichle and Mintun, 2006).

In the fMRI field, the spontaneous modulation of the blood oxygen level dependent (BOLD) signal, which cannot be attributed to the experimental paradigm, has been viewed for many years as "noise" and is usually minimized through averaging. Several groups observed by means of functional connectivity analyses that spontaneous BOLD fluctuations appear not to be just random noise, but are specifically organized in functionally relevant *resting-state networks* (RSNs) (Biswal et al., 1995; Lowe et al., 1998; Cordes et al. 2001; Raichle et al., 2001; Greicius et al., 2003; Fransson, 2005; Fox et al. 2006). Even so, it is still a matter of discussion to what extent the observed fluctuations in the RSNs of the resting fMRI signal are a direct consequence of neuronal activity or whether they are low-frequency artifacts due to other processes (physiological and scanner related artifacts). A growing body of evidence suggests that despite being able to detect about a dozen spatially consistent RSNs across subjects (Fox and Raichle, 2007), fMRI alone, as an *indirect* measure of neural activity, is not well suited to assess the functional significance of these RSNs. A further disadvantage is that the BOLD signal changes are

* Corresponding authors. Neuropsychiatric Research Laboratory Dept. of Psychiatry, Heinrich-Heine University, Bergische Landstr. 2, 40629 Duesseldorf, Germany. Fax: +49 211 922 2759.
E-mail addresses: Francesco.Musso@lvr.de (F. Musso), Jurgen.Brinkmeyer@lvr.de (J. Brinkmeyer).
[1] These authors contributed equally.

1053-8119/$ – see front matter © 2010 Published by Elsevier Inc.
doi:10.1016/j.neuroimage.2010.01.093

delayed and temporally blurred with respect to the underlying neural events.

On the contrary, electroencephalography (EEG) is a *direct* measure of the activation status of large cooperating neuronal assemblies. In the electrophysiology field, "spontaneous activity," has been observed already from the earliest recordings by Berger in the late twenties. The posterior 8–12 Hz oscillations were named "alpha rhythm" and it is the most prominent EEG rhythm during the awake resting state with closed eyes (Berger, 1929).

There is good evidence that spontaneous electrophysiological activity is coherently expressed in larger neuronal populations (Arieli et al., 1996; Tsodyks et al., 1999; Salek-Haddadi et al., 2003). Resting EEG activity appears to be macroscopically organized across the brain and fluctuates coherently in specific brain circuits (Laufs, 2008). This might be related to fluctuations of specific mental activities corroborating the concept of a "default mode" of brain function as proposed by imaging studies (Raichle et al., 2001). EEG is able to provide information on the subjects' vigilance and to some degree the *state of mind*, endowed in the frequency domain and electric field potential topography. Despite its richness of direct information about the neuronal activity, EEG is deficient with regard to the spatial localization of sources and space resolution.

The obvious solution to combine the two measurements was at first motivated by the clinical interest in mapping changes in neural activity associated with epileptic discharges onto MRI images of brain anatomy (Ives et al., 1993). Borrowing a metaphor from Laufs, epilepsy researchers adopting simultaneous multimodal experiments were forced to "marry the blind and the lame," in order to explore neural processes which cannot be monitored or recalibrated by neurophysiological behavior such as resting brain activity (Laufs, 2008; Laufs et al., 2008). Recently the technical aspects of recording electrophysiological data simultaneously with fMRI have rapidly progressed thanks to dedicated EEG hardware and artifacts removal procedures (Laufs et al., 2008) so that it has become possible to exploit both signals to extract the best temporal and spatial resolution.

Most multimodal studies on spontaneous brain activity use regressors for the model derived from convolving the power time courses of the frequency bands of interest with a canonical hemodynamic response function. As expected, the first EEG/fMRI investigations of this kind were concerned with the BOLD correlates of alpha rhythm, which traditionally desynchronize with engagement in attention demanding tasks on the one hand and with sleepiness on the other. The majority of those experiments, in line with electrophysiological animal studies, identified thalamic BOLD activity to be positively and occipital–parietal areas to be inversely correlated with alpha oscillations (Goldman et al., 2002; Moosmann et al., 2003; Laufs et al. 2003a,b; De Munck et al., 2007). By identifying inverse relationships, those studies identified brain regions that increase their activity in the absence of marked alpha activity. The failure to identify an average cortical BOLD signal pattern which is positively correlated with alpha power (except for the thalamic activation) may be explained by the fact that fMRI group analysis fails to detect non-uniform brain activity during periods of prominent alpha oscillations (Laufs et al., 2006) suggesting that for a more comprehensive assessment of neural oscillations broader EEG spectral properties should be incorporated into the analysis procedure. Notably, performing the same type of analysis as for alpha power with frequency oscillations in the "beta" band (13–30 Hz), led to positive correlation of β-2 power (17–23 Hz) with the default mode network (Laufs et al., 2003b). Through a sophisticated approach, which combines data-driven fMRI analysis such as independent components analysis (ICA) to identify RSNs and which correlates the representative time courses to EEG bands between 1 and 50 Hz averaged across the entire scalp, Mantini et al. (2007) demonstrated that each of these networks could be generally associated with more than one specific electrical oscillation frequency band. Moreover, showing that different RSNs might exhibit positive as well negative correlation with α and β-oscillations, the work of Mantini et al. (2007) contradicts in part previous findings about the positive correlation of β-2 power band with the default mode network. So far, it appears that similar EEG frequency bands recorded at the scalp can be associated with different fMRI-generated spatial maps, while BOLD fluctuations of a distinct single network may correspond to diverse EEG patterns (Laufs et al., 2008). One potential reason for this observation may lie in the temporo-spatial properties of BOLD and surface EEG signals which are generated differently. Indeed, the EEG has been traditionally decomposed into a series of fixed broad spectral bands (delta, theta, alpha, beta, gamma) based more on history and discovery than on a theoretical framework. This way to look at the data, although computationally convenient, may obscure the fact that the sources of each of these characteristic oscillations may or may not be unique (Szava et al., 1994).

In the present study we start from the assumption that a complex spectral signature is more likely to characterize the hemodynamic fluctuations at rest (Mantini et al., 2007), and that isolating specific frequency bands might result in an over-simplification of data space. Pioneering work by Lehmann (1987) introduced a novel method to investigate the time domain of the EEG, the so-called "EEG segmentation" which focuses on transient EEG events and identifies and quantifies brain electric *microstates* as time epochs with quasi-stable field topography. A brain microstate is defined as a functional/physiological state of the brain during which specific neural processes occur. It is characterized uniquely by a fixed spatial distribution of active neuronal generators with time varying intensity. Brain electrical activity is modeled as being composed of a time sequence of non-overlapping microstates represented as normalized vectors constituted by scalp electric potentials with variable duration (Pascual-Marqui et al., 1995). In addition, we suggest that EEG segmentation techniques might prove particularly well suited to explore complex neuronal networks, identifying direct neuronal activity and associating it with a specific source distribution at a given time point. In the present study, we modeled the hemodynamic response function (HRF) using the microstates as regressors for the BOLD fluctuations during *relaxed wakefulness*.

Materials and methods

Subjects and resting condition

Eleven healthy, male, right-handed subjects with a mean age of 29.5 years (SD ± 9.33 years) were recruited from the environment of the local university (students or staff). Subjects had no history of neurological or psychiatric disease and did not take any medication that could affect the experiment. All participants gave written informed consent to participate in the study which was approved by the local ethics committee. Subjects were instructed simply to lie still in the scanner with closed eyes and refrain from falling asleep.

EEG data acquisition

EEG data were recorded using a 32-channel MR compatible EEG system (Brain Products, Gilching, Germany). The EEG cap (BrainCap MR, EasyCap GmbH, Breitbrunn, Germany) consisted of 30 scalp electrodes distributed according to the 10–20 system and two additional electrodes, one of which was attached to the subjects' back for recording the electrocardiogram (ECG), while the other was attached on the outer canthi of the left eye for detection of ocular artifacts. Data were recorded relative to an FCz reference and a ground electrode was located at Iz (10–5 electrode system, Oostenveld and Praamstra, 2001). Data were sampled at 5000 Hz, with a bandpass of 0.016–250 Hz. Impedance at all recording electrodes was less than 10 kΩ. The vigilance state was monitored continuously by observing

the EEG on the screen (Brain Vision RecView, Gilchingen) and the subject to make sure that the subject did not become drowsy. When a subject became drowsy, an acoustical signal was given; the portion of EEG influenced by drowsiness was marked and excluded from further analysis.

EEG data analysis

Raw EEG data were processed offline using BrainVision Analyzer version 1.05 (Brain Products, Gilching, Germany). Gradient artifact correction was performed using modified versions of the algorithms proposed by Allen et al. (2000), where a gradient artifact template is subtracted from the EEG using a baseline corrected sliding average of 20 MR-volumes. Data were then down-sampled to 250 Hz. Following gradient artifact correction, the data were corrected for cardioballistic artifacts. For this purpose, an average artifact subtraction method (Allen et al., 1998) was implemented in Brain Vision Analyzer. This method involves subtracting the artifact on a second by second basis using heartbeat events (R peaks) detected in the previous 10 s. As such it requires accurate detection of R peaks which is aided by the employment of a moving average low pass filter and a finite impulse response high pass filter (for details, see Allen et al., 1998). In the present study, the R peaks were detected semi-automatically, with manual adjustment for peaks misidentified by the software. To average the artifact in the EEG channels, the R peaks are transferred from the ECG to the EEG over a selectable time delay. The average artifact was then subtracted from the EEG. Once gradient and cardioballistic artifacts had been removed, the data were then inspected for artifacts resulting from eye blink or other muscular sources, and any epoch containing a voltage change of more than 150 μV was rejected.

For analyzing the resting EEG data, we decided to regard at brain electric activity as a series of scalp maps of momentary potential distributions which change over time its geometric distribution: the "landscape" (Lehmann, 1971, 1987). The series of momentary potential distribution maps can then be clustered into successive time epochs ("microstates") that are defined by quasi-stable landscapes of the brain electric field (Brandeis and Lehmann, 1989; Fingelkurts, 2004; Lehmann and Skrandies, 1980; Lehmann et al., 1987, 1998; Michel et al., 2004; Pascual-Marqui et al., 1995; Wackermann et al., 1993; Zhou et al., 1999). The spontaneous fluctuations of EEG recorded activity are classified as belonging to some microstate, thus producing a natural segmentation of resting brain electrical activity. Individual resting EEG datasets were segmented with a specific module in sLORETA (standardized low resolution electromagnetic tomography) software package (Pascual-Marqui et al., 1994; Pascual-Marqui, 1999; Pascual-Marqui, 2002) in which microstates are represented as normalized vectors constituted by scalp electric potentials due to the underlying generators (Figs. 1 and 2). The algorithm implemented for estimating the microstates, is based on a modified version of the classical *k-means clustering* method, in which cluster orientations are estimated (Pascual-Marqui et al., 1995).

In order to display the electrical generators on the scalps alongside the BOLD activation maps we performed a current density analysis in 3-D Talairach space of the resting EEG microstates using sLORETA. This approach is based on the physiological observation of coherent firing of neighboring neurons and assumes that the smoothest of all activity distributions is most plausible. sLORETA images represent the standardized electrical activity at each voxel as amplitude of the computed current source density ($\mu V/cm^2$). As a consequence of the smoothness constraint, the characteristic feature of the resulting solution is a relatively low spatial resolution with a "blurred-localized" image of a point source. The version of LORETA employed in the present study used the digitized Talairach atlas estimating the current source density distribution for 40 ms epochs of brain electrical activity (Pascual-Marqui, 2002).

In the current implementation of sLORETA, computations were made in a realistic head model (Fuchs et al., 2002), using the MNI152 template (Mazziotta et al., 2001), with the three-dimensional solution space restricted to cortical gray matter, as determined by the probabilistic Talairach atlas (Lancaster et al., 2000). The standard electrode positions on the MNI152 scalp were taken from Jurcak et al. (2007) and Oostenveld and Praamstra (2001). The intracerebral volume is partitioned in 6239 voxels at 5 mm spatial resolution. Thus, sLORETA images represent the standardized electric activity at each voxel in neuroanatomic Montreal Neurological Institute (MNI) space as the exact magnitude of the estimated current density.

Only voxels significant at $p = 0.01$ or $p = 0.05$ level after correction for multiple comparisons were retained, i.e., the significance of changes in activity compared to baseline was assessed using non-parametric analyses adapted to source comparisons and implemented in sLORETA which correct for multiple comparisons (statistical non-parametric mapping, SnPM, Holmes et al., 1996).

Statistical factor analysis

In order to classify similar topographies across all subjects a *factor analysis* was conducted on the EEG microstates using the SPSS (SPSS Inc, Chicago, IL, USA) statistical analysis software. Factor analysis is a statistical method used to describe variability among observed variables in terms of fewer unobserved variables called factors. The

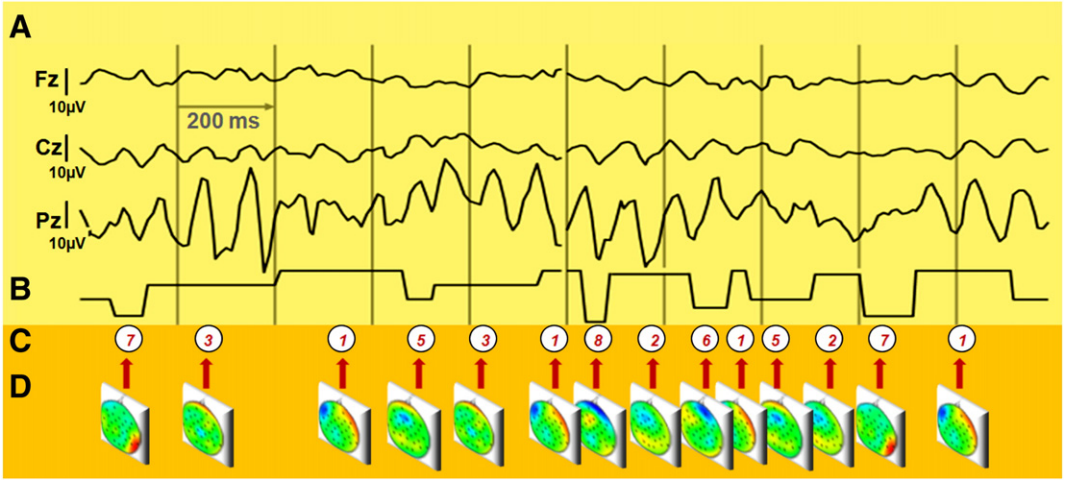

Fig. 1. EEG microstate segmentation. (A) Partial stack plot of one subject's resting EEG obtained from electrodes position Fz, Cz and Pz (1st, 2nd and 3rd rows). B) Linear representation of EEG microstates duration. (C) sLORETA numeric classification. (D) Correspondent quasi-stable electric field topography or microstates.

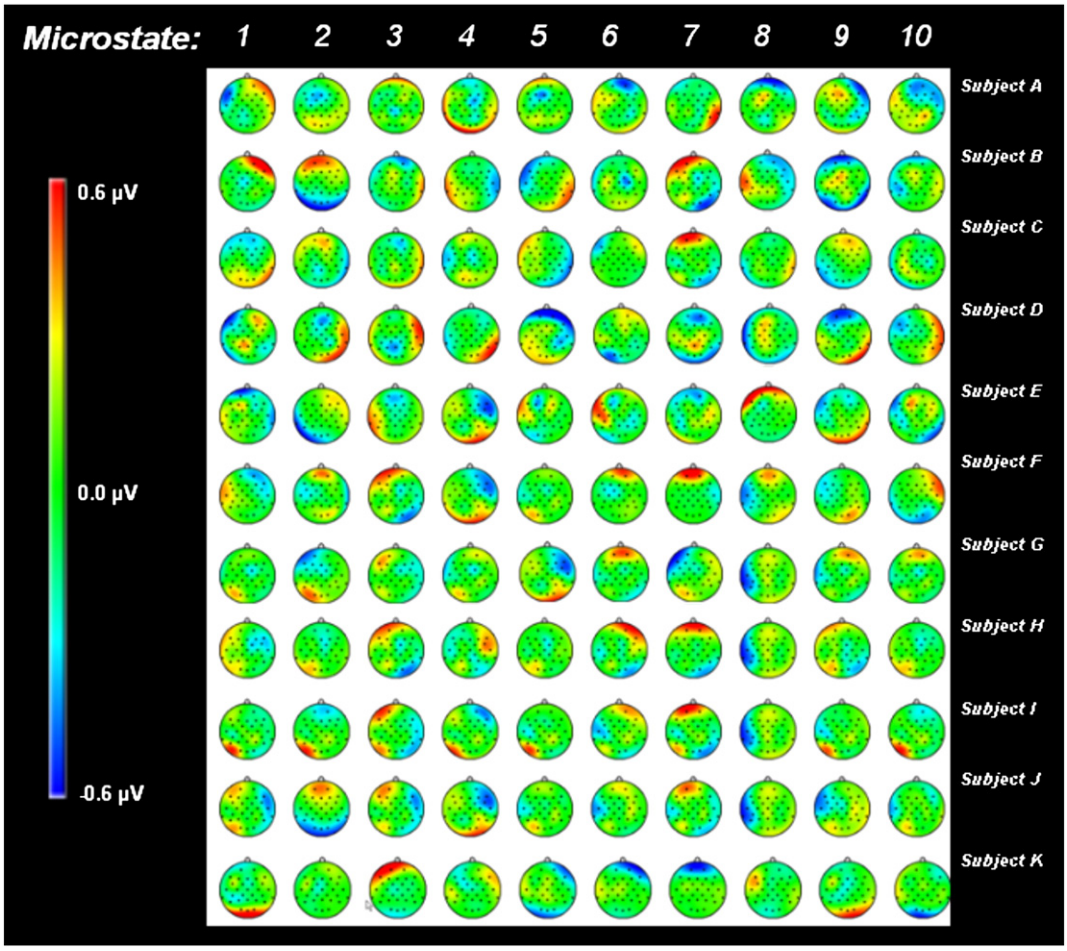

Fig. 2. EEG microstate overview. Overview of the quasi-stable electric field landscapes (or microstates) across all subjects, obtained after 200 iterative calculations with sLORETA for each EEG dataset (maximum variance amount accounted: 89%). In each subject 10 recurrent quasi-stable scalp electric topographic distributions were identified and are here depicted by mean of field maps. Notice that sLORETA classify the segments according to the amount of explained variance for each individual subject hence the heterogeneous field maps across subjects.

observed variables are modeled as linear combinations of the factors, plus "error" terms. The information gained about the interdependencies can be used later to reduce the set of variables in a dataset. Factor analysis is related to principal component analysis (PCA) but not identical. Because PCA performs a variance-maximizing rotation of the variable space, it takes into account all variability in the variables (Tipping and Bishop, 1999). In contrast, factor analysis estimates how much of the variability is due to aggregation factors or common factors ("communality"). The analysis showed that seven aggregation factors were able to explain 80.5% of the EEG data variance across subjects. Thus, by grouping the different microstates across all subjects, it was possible to search for correspondence of BOLD and EEG signal on the group level as well. Fig. 3 depicts in details those aggregation factors as CSD maps, percentage of explained global variance, mean microstate duration in milliseconds, and spectral signature.

fMRI data acquisition

Functional MR-images were acquired using a 3T scanner (Trio, Siemens, Erlangen, Germany). In order to avoid head movements, the head of each subject was tightly fixated during the scanning procedure with vacuum cushions and sponge pads. Using echo planar imaging (EPI), 200 volumes were obtained applying the following EPI parameters: 42 slices, no gap, slice thickness 3 mm, FOV 192×192 mm, matrix 64×64, repetition time 3400 ms, echo time 40 ms, flip angle 90°. To facilitate localization and co-registration of functional data, structural scans were acquired using T1-weighted MRI sequences (magnetization prepared rapid gradient echo (MP-RAGE): TR/TE = 1700/3.5 ms, flip angle = 9°, 208 sagittal slices, FOV 240×195 mm, matrix 320×260, voxel size 0.75×0.75×0.75 mm.

fMRI analysis

fMRI analysis was performed with FSL (FMRIB's Software Library, www.fmrib.ox.ac.uk/fsl). The following pre-processing procedure was applied: employing different modules of the FSL-software package, we conducted motion correction using MCFLIRT (Jenkinson et al., 2002), non-brain removal using BET (Smith, 2002), spatial smoothing using a Gaussian kernel of FWHM = 5 mm, mean-based intensity normalization of all volumes by the same factor, and high pass temporal filtering (sigma = 50 s). Whole brain general linear model (GLM) time series statistical analysis of individual data sets was carried out using FILM (FMRIB's improved linear model) with local autocorrelation correction (Woolrich et al., 2001). Registration of functional images to high-resolution structural images was done with FLIRT (Forman et al., 1995; Jenkinson et al., 2002).

Exploratory BOLD independent components analysis (ICA)

Since we are dealing with resting bold fluctuation and not with task related activations, artifacts represent a challenging confounding factor, which often account for a large part of data variance, leading to a problematic data interpretation. A classic approach to deal with such confounds is to model them (e.g. motion-related noise) within the GLM (Friston et al., 1996). However following this procedure only the components of the main explanatory variables (EVs) that are orthogonal to the confound EVs will be used in determining significance of

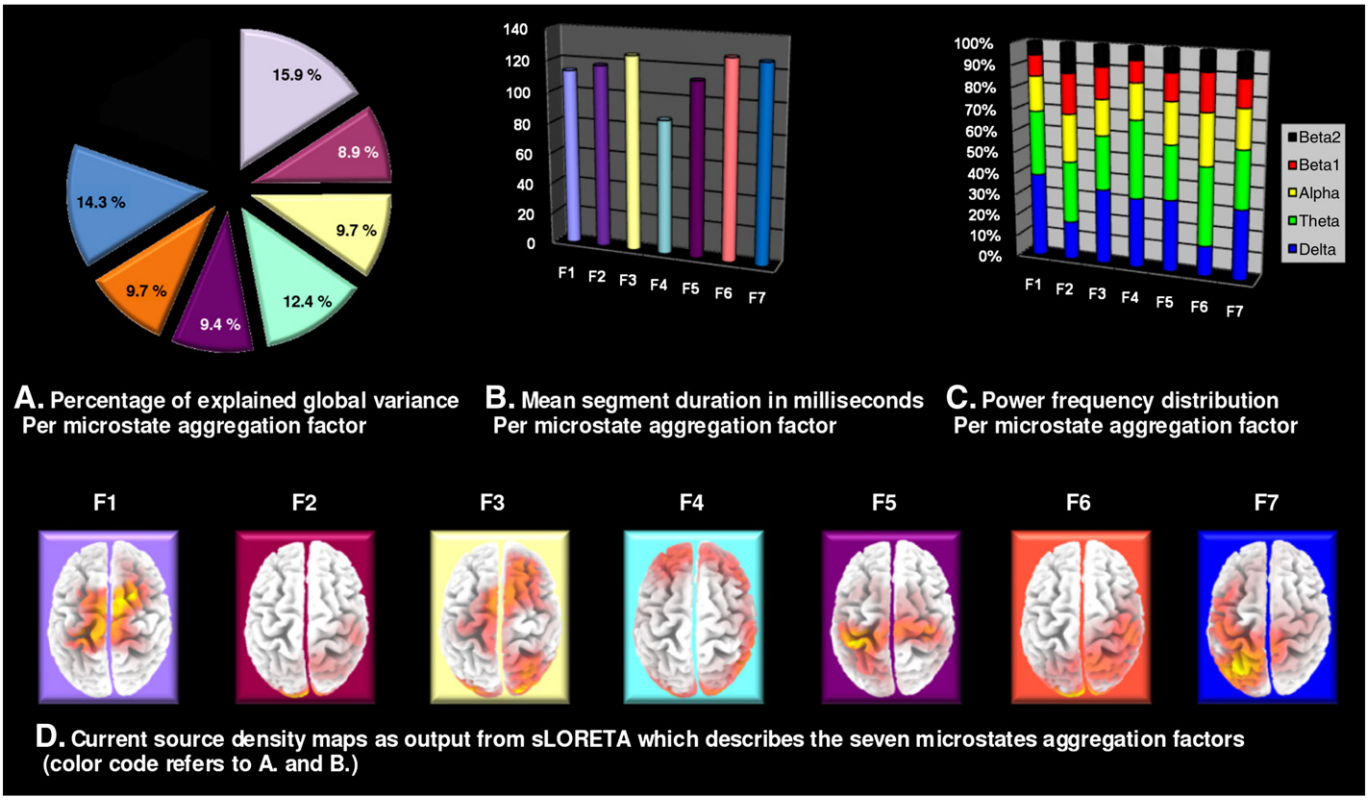

Fig. 3. Statistical factor analysis on the microstates. Statistical factor analysis conducted on the EEG microstates (SPSS Inc, Chicago, IL, USA). The figure shows the seven aggregation factors which were able to explain 80.5% of the EEG data variance grouping the EEG segments across all subjects. The figure depicts in detail those aggregation factors as: A. percentage of explained global variance; B. mean segment duration in milliseconds; C. power spectrum properties; D. sLORETA CSD maps ($\mu V^2/cm^2$). A, B and D follow the same color code.

the effects of interest. At a conceptual level, the notion of orthogonality (i.e. uncorrelatedness) is overly restrictive (Beckmann et al., 2001; Beckmann et al., 2005). Within the temporal domain, signal often spans the entire length of an experiment. If the 'true' temporal characteristics of different signals are partially correlated a decomposition which enforces orthogonality in the temporal domain will necessarily misrepresent at least one of the time series in order to satisfy the constraint (Beckmann et al., 2005). For this reason to deal with such confounding factors we opted for a single-session BOLD ICA to identify and then "clean up" the EPI datasets from gradient, cardioballistic and movement related artifacts, searching for ICs which are independent but not necessarily orthogonal. Analysis was carried out using probabilistic independent component analysis or *PICA* (Beckmann and Smith, 2004) as implemented in MELODIC (Multivariate Exploratory Linear Decomposition into Independent Components) Version 3.05, part of FSL (FMRIB's Software Library, www.fmrib.ox.ac.uk/fsl). The following data pre-processing was applied to the input data: masking of non-brain voxels; voxel-wise de-meaning of the data; normalization of the voxel-wise variance; pre-processed data were whitened and projected into a 13-dimensional subspace using probabilistic principal component analysis where the number of dimensions was estimated using the Laplace approximation to the Bayesian evidence of the model order (Minka, 2000; Beckmann and Smith, 2004). The whitened observations were decomposed into sets of vectors which describe signal variation across the temporal domain (time courses) and across the spatial domain (maps) by optimizing for non-Gaussian spatial source distributions using a fixed-point iteration technique (Hyvärinen, 1999). Estimated Component maps were divided by the standard deviation of the residual noise and thresholded by fitting a mixture model to the histogram of intensity values (Beckmann and Smith, 2004). The solution we adopted was an hybrid one, using both the visual inspection of the ICs for confounds which were not motion related and the correlation of the rigid body displacement parameters (three translation and three rotation parameters) with the IC time courses as objective approach.

Visual inspection of the artifact ICs

Independent components were qualitatively selected by visual inspection searching for anatomically relevant areas across subjects, potentially depicting functionally relevant resting-state networks. Components excluded from further analysis show clearly interpretable distinct artifact patterns. We referred to the work of Beckmann et al. (2005) and Beckmann and Smith (2005) for examples of the spatial/frequency patterns of "non motion-related" noise sources such as: eye-related artifacts, field inhomogeneity, high-frequency noise, slice drop-outs and gradient instability. At our TR (3.4 s) the temporal signature of the cardiac and respiratory cycles become aliased and no longer identifiable in the time course of the ICs. Nevertheless tensor ICA demonstrated to be capable to separate those IC with clearly identifiable patterns in both the spatial and the frequency domain (Beckmann et al., 2005; Beckmann and Smith, 2005; Damoiseaux et al., 2006; De Luca et al., 2006).

Regression analysis ICs time courses vs movement regressors

In parallel to a "visual inspection" of the independent components (ICs), we performed a post-hoc regression analysis on the estimated six movement regressors (three translation and three rotation parameters estimated by MCFLIRT, FMRIB's Software Library) in order to check whether or not a given independent component was movement related. MELODIC performed a simple *F*-test on the estimated time course and the total model fit. An *F* value of 20 or more was considered sufficient to classify an IC as artifact. The artifact components once identified were removed using the MELODIC tool "reg_filt" (FMRIB's Software Library).

EEG informed fMRI analysis

For the analysis of the resting functional data at the single subject level, we treated the EEG microstates as single trial "event related potentials (ERPs)" in an event related design, considering them as explanatory variables in the GLM analysis. However instead of performing a conventional analysis of the data with a constant impulse function positioned at the onset of a specific microstate, we modeled the input function using the onset time, and the duration of each EEG microstate (i.e. quasi-stable scalp electric topographic distribution or "microstate") and convolved them with a gamma hemodynamic response function, adopting a variable epoch model (Warbrick et al., 2009). By informing the GLM with the EEG parameters we gain a better fit of the model thus making a more accurate prediction about brain resting-state fluctuations. The idea behind this choice is that a longer microstate would reflect a more stable topographic distribution and thus predict a stronger BOLD response, so this approach should model activation sensitive to microstates time variability.

Single subject data "cross validation" through BOLD ICA

The analysis to identify the RSNs was carried out using probabilistic independent component analysis or *PICA* instead of a classic "activation-seeded" correlation analysis. The latter is based on the hypothesis that in resting data, the low-frequency temporal fluctuations are correlated in regions which are functionally associated (Biswal et al., 1995; Lowe et al., 1998). In this approach, a statistical map is generated by calculating the correlation of all time courses in the resting data against the time course of the seed voxel in order to find a temporally consistent resting network. The applicability of this technique, however, is limited by the fact that seed-voxel-based analysis relies on the time course at the seed voxel location being a 'good' representative for the set of correlated voxels under rest. The choice of the seed voxel is rather arbitrary and can be biased by different types of fMRI noise. For resting fMRI analysis, PICA has proven able to reveal activation patterns that are mostly limited to grey matter and that are spatially consistent across subjects, clearly identifying networks of functional significance including areas such as visual, sensory or motor cortex (Beckmann et al., 2005; Damoiseaux et al., 2006; De Luca et al., 2006). Starting from these considerations we opted for an ICA method to identify RSNs at the single subject level and then correlate them to our EEG driven GLM analysis looking for similarities. Our hypothesis is that the different activity of brain neural populations, which underlie the different map landscapes of brain potential distributions on the scalp surface (i.e., account for the different microstates), should be reflected in some of those activity patterns, i.e., RSNs. In order to test this hypothesis and using MELODIC (FMRIB's Software Library), we performed a post-hoc regression analysis on estimated time courses (i.e., microstate regressors) to identify whether or not a given BOLD IC was related with a specific recurrent "landscape" of the brain electric field, i.e. might considered "functionally similar." MELODIC performed a simple *F*-test on the estimated time course and the total model fit. BOLD ICs unthresholded, Gaussianized spatial maps, selected on the basis of their functional similarity were than compared with the EEG-modulated GLM statistical spatial maps by using simple Pearson correlation as measure of "spatial similarity" (Smith et al., 2009).

Group level fMRI analysis

Each microstate regressor was weighted according to one of the previously mentioned seven aggregation factors and was included into a design matrix comprehensive of all subjects and all microstates. Seven group level mixed effect analyses were then conducted using FLAME (FMRIB's local analysis of mixed effects) (Behrens et al., 2003) with spatial normalization to MNI (Montreal Neurological Institute) space and applying a cluster significance threshold of $Z>2$ (Forman et al., 1995; Friston et al., 1996; Worsley et al., 1992). For visual display of the group results, *Z*-maps of the functional data were imported to MRIcron (Rorden et al., 2007).

Group level data "cross validation" through multi-session temporal concatenation PICA

Analysis was carried out using "multi-session temporal concatenation PICA" (Beckmann and Smith, 2004) as implemented in MELODIC (Multivariate Exploratory Linear Decomposition into Independent Components) Version 3.05, part of FSL (FMRIB's Software Library, www.fmrib.ox.ac.uk/fsl). Employing different modules of the FSL-software package, we conducted motion correction using MCFLIRT (Jenkinson et al., 2002), non-brain removal using BET (Smith, 2002), spatial smoothing using a Gaussian kernel of FWHM = 5 mm, mean-based intensity normalization of all volumes by the same factor, and high pass temporal filtering (sigma = 50 s). Registration of functional images to high-resolution structural images was done with FLIRT (Forman et al., 1995; Jenkinson et al., 2002). Registration from the high-resolution structurals to MNI152 standard space was achieved by using FLIRT affine registration. All subjects' 4D FMRI time series data were transformed into standard space at $2\times2\times2$-mm resolution, by using the registration transformations derived as described above. Than a single 2D ICA run on the concatenated data matrix (obtained by stacking all 2D data matrices of every single data set on top of each other) was performed. This approach is recommended in cases where one is looking for common spatial patterns but cannot assume that the associated temporal response is consistent between sessions/subjects, like analysis of data acquired without stimulation (such as resting-state fMRI). ICA was run with MELODIC estimating the optimal dimensionality of the data; this aids in achieving ICA convergence stability. All ICA spatial maps were originally Gaussianized via a normalized mixture-model fit, and then thresholded at $Z=2$ (an additional $Z=-2$ statistical map is superimposed to show also the negative correlation when present) for all produced maps.

Results

EEG microstates segmentation

We conducted up to 200 iterative calculations with sLORETA for each EEG dataset which accounts for the maximum variance amount (i.e. 89%). In each subject 10 recurrent quasi-stable scalp electric topographic distributions were identified and each EEG dataset was segmented accordingly. Each microstate describes a momentary stable topographic potential distribution which is characterized by a specific occurrence (see the example in Fig. 1), a mean duration of 119.72 ms (SD: ±64.11 ms) and a mean occurrence rate (see Table 1). A complete overview of the microstates landscapes across all subjects is depicted in Fig. 2.

ICA BOLD artifact removal

The BOLD GLM analysis greatly benefited from the ICA BOLD denoising. After the exploratory ICA decomposition a mean of 36.5 ICs

Table 1
Mean occurrence rate (in percent) of the EEG segments across all subjects clustered via factor analysis.

EEG segment	1	2	3	4	5	6	7	8	9	10
Mean occurrence rate (%)	8.65	4.29	9.27	14.97	4.22	7.39	14.17	10.70	21.50	4.84
SD	0.47	0.82	0.74	1.05	0.77	0.94	1.00	1.03	0.98	0.66

Table 2
Number of total BOLD independent components (ICs) (mean: 36.5 ± 6.6 SD), number of movement related ICs (mean: 15.9 ± 5.4 SD) and total number of artifact related ICs (mean: 25.6 ± 6.5 SD) per subject, estimated in the exploratory ICA BOLD decomposition as implemented in MELODIC (Multivariate Exploratory Linear Decomposition into Independent Components) Version 3.05, part of FSL (FMRIB's Software Library, www.fmrib.ox.ac.uk/fsl).

Subject	Total ICs	Movement related ICs	Total artifact related ICs
A	37	11	20
B	32	11	20
C	33	15	25
D	28	9	16
E	40	19	28
F	41	23	34
G	34	22	29
H	33	11	24
I	30	14	20
J	50	16	29
K	44	24	37

(SD: ±6.6) per subject was estimated, of which a mean of 25.6 ICs (SD: ±6.5) per subject was classified as artifacts after visual and a post-hoc regression analysis of the estimated IC with the six movement regressors (cutoff $F \geq 20$). Most of the discarded components were motion related (15.9 ± 5.4 SD) and thus objectively identified via correlation of the rigid body displacement parameters with the BOLD IC time courses (see Table 2 for detailed information). In case of a doubtful component we adopted a conservative approach keeping the IC rather than discarding it. In most cases the artifacts removal was associated with a broader and stronger activation in known RSNs. Fig. 4 shows an example of how movement related artifacts and other noise sources (of physiological and non physiological origin) might submerge the signal of interest in resting fMRI.

EEG microstates informed BOLD modeling and ICA BOLD cross validation analysis

Using the EEG microstates as regressors for the GLM analysis of resting fMRI, significant BOLD-responses were present in all 11 subjects. The results for four selected single subjects at rest are visually summarized in Fig. 5. For displaying purposes, we included a sLORETA CSD to illustrate the specific electrophysiological landscape or microstate used to inform the fMRI analysis (Fig. 5A). Fig. 5B shows the BOLD activation maps (Z values) elicited using specific EEG microstates to inform the GLM analysis.

In the depicted examples the occurrence and duration of the EEG microstates included in a variable epoch GLM model revealed significant BOLD cortical resting fluctuations that have been identified as RSNs in numerous previous studies.

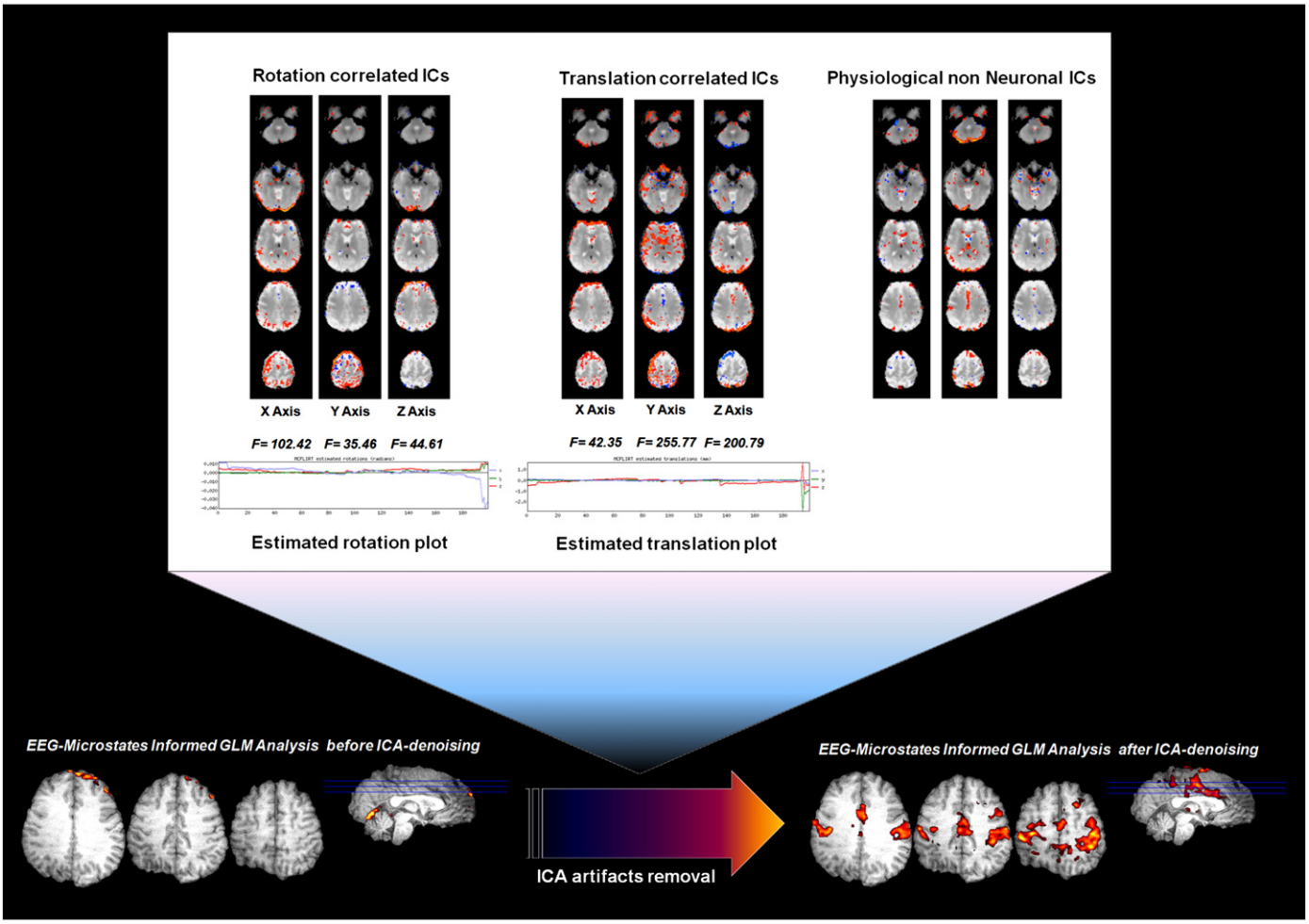

Fig. 4. ICA BOLD denoising. Example of exploratory ICA decomposition as denoising method for one representative subject. The left upper part of the figure shows movement related ICs classified via post-hoc regression analysis with the six movement regressors, three rotation related regressors (correspondent plot in radians along the x, y and z axis) and three translation related regressors (correspondent plot in mm along the x, y and z axis) all showed F values far above the cutoff ($F \geq 20$). The right upper part of the figure shows other physiological non neuronal ICs identified by mean of visual inspection. The artifacts ICs removal in this case was associated with a broader and stronger activation in known RSNs, showing how the signal of interest in resting fMRI was submerged (lower part of the figure) from other noise sources.

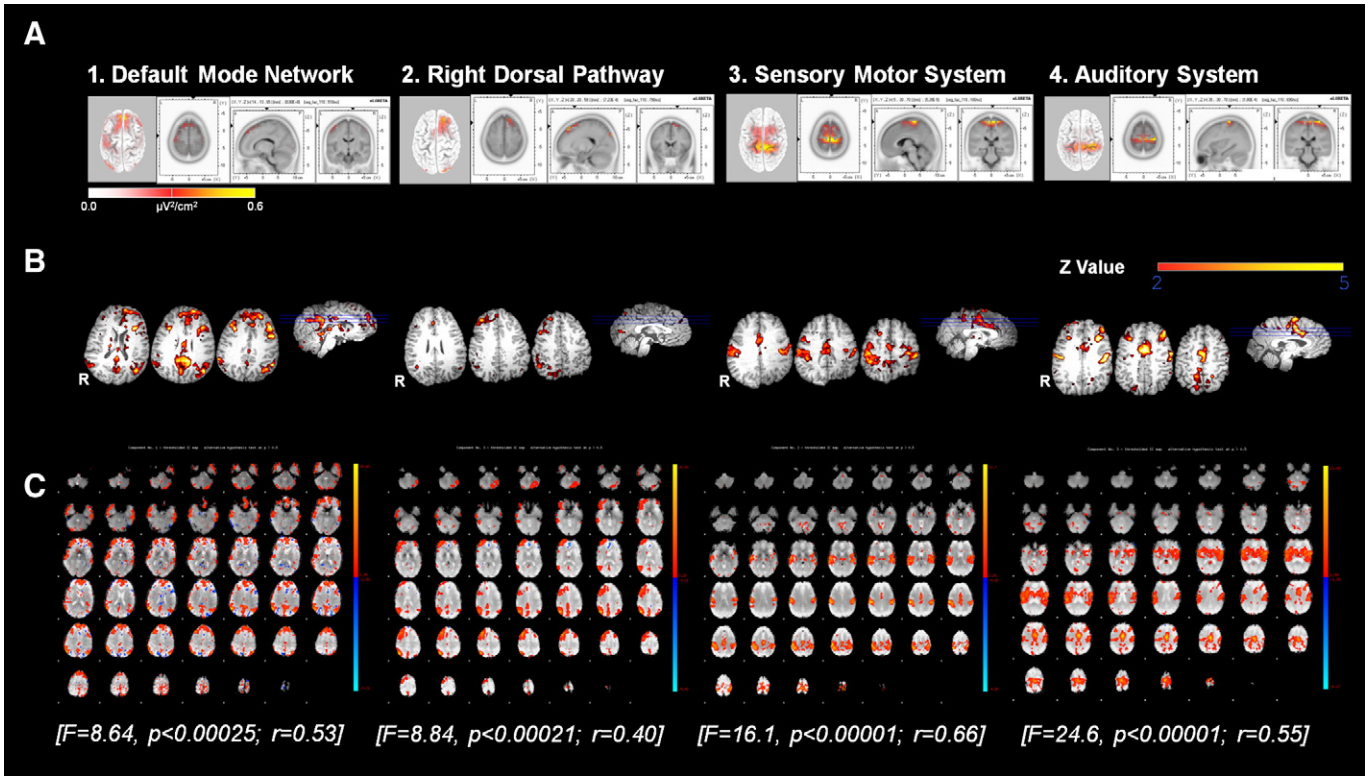

Fig. 5. EEG microstates informed fMRI analysis and ICA BOLD cross validation analysis. The figure shows through different imaging and analysis modalities four selected RSNs elicited in four different subjects. In B all images have been coregistered into the space of the MNI template, in B and C the images are shown in radiological convention. A. sLORETA CSD maps ($\mu V2/cm^2$) to show the specific electrophysiological landscape or microstate used to inform the fMRI analysis in four selected single subject at rest. In each column on the left a CSD map projected onto a 3D Talairach model of the brain while on the right axial, sagittal and coronal views of a microstate CSD map is shown. B. BOLD activation maps (Z values) elicited using the EEG microstates displayed in panel A to inform the GLM analysis in four selected single subject at rest. Axial slices are taken on the level of the PCC and ACC. From left to right the elicited RSNs: default mode network, right dorsal pathway, sensory motor system, and auditory system. Cluster-corrected threshold $Z=2$, $p=0.05$. R = right. C. Different PICA-estimated resting patterns used as cross validation for EEG informed fMRI. Axial slices of different spatial maps (BOLD ICs as output of MELODIC) associated with low-frequency resting patterns at the single subject level significantly correlated with the microstate regressors as expression of "functional similarity" and Pearson r correlation coefficient as expression of "spatial similarity" (F, p and r values are expressed in parenthesis at the bottom).

Default mode network: activation in this cluster encompassed anterior and posterior cingulate, middle frontal gyrus, angular gyrus, supramarginal gyrus, and thalamus as described by Raichle et al. (2001) and Greicius et al. (2003). Additional activation was observed in temporal fusiform cortex, frontal pole, caudate and amygdala (Fig. 5B_1).

Right dorsal pathway: primarily lateralized activations in bilateral intracalcarine cortex, right lateral occipital complex, right superior parietal cortex, right supramarginal gyrus, and right middle and superior frontal gyri (Fig. 5B_2) as described by Beckmann and Smith (2004), Beckmann et al. (2005) and De Luca et al. (2006).

Sensory motor system: this pattern of activation corresponds to that seen in bimanual motor tasks as identified in previous RSN studies (Biswal et al., 1995) and includes activation in pre- and post-central gyri extending from the superior temporal gyrus, deep into the Sylvian fissure and up to the medial wall of the interhemispheric fissure, including the ACC and SMA (Fig. 5B_3).

Auditory system: this activation pattern covered primary and secondary auditory cortices, including Heschl's gyrus, planum polare and planum temporale, the superior temporal gyrus and insular cortex (Rivier and Clarke, 1997; Rademacher et al., 2001), and additional activation was observed in the anterior cingulate cortex, middle frontal gyrus, frontal pole and supramarginal gyrus (Fig. 5B_4). Visual inspection suggests that the CSD maps show a good correspondence to fMRI Z-maps as displayed in Fig. 5A.

Using an entirely data-driven fMRI approach to cross validate the results (BOLD PICA), we found that at the single subject level the same activation pattern elicited by the microstate-modulated GLM analysis is also "captured" in BOLD ICs showing both a significant F value in the post-hoc regression analysis on the microstate regressors as expression of "functional similarity" as well as a high score in the Pearson r correlation coefficient as expression of "spatial similarity." Fig. 5C illustrates the ICs as output from MELODIC (FMRIB's Software Library) related to the depicted microstates (F, p and r values are expressed in parenthesis at the bottom).

Results are also summarized in Table 3. In addition, to give a complete overview about the results a table is available as Supplementary Table 1. This table reports all the brain regions (according to Harvard–Oxford structural atlases) in which the electroencephalogram microstate regressors showed a positively correlated BOLD signal at the single subject level. Here active voxels are grouped in clusters ($Z>2.3$) of decreasing dimensions with the coordinates of local Z-maxima according with FEAT (part of FSL, FMRIB's Software Library, www.fmrib.ox.ac.uk/fsl). To allow also a visual overview we created high-resolution images as Supplementary Fig. 1a–j about the 55 microstates which showed a positively correlated BOLD signal at the single subject level. Each picture contains the "landscape" (quasi-stable current scalp distribution in μV), the elicited BOLD GLM Z-map (clustered at $Z>2.3$ and thresholded at $Z=2$) and the functional related BOLD IC thresholded at $Z=2$ (an additional $Z=-2$ statistical map is superimposed to show also the negative correlation when present) selected on the basis of the F value. The Pearson r coefficient as measure of spatial similarity is also reported.

EEG informed resting fMRI group analysis and group ICA BOLD cross validation analysis

At the group level mixed effect analysis, in which the design matrix included all microstates each weighted according to the correspon-

Table 3
EEG microstates classified according to sLORETA which elicited BOLD activation in GLM modeling (FMRIB's Software Library. www.fmrib.ox.ac.uk/fsl). BOLD ICs from the probabilistic ICA decomposition were chosen on the basis of their "functional similarity," i.e. correlation in the time domain, with the microstates (a simple *F*-test on the ICs time courses and the total model fit to EEG microstates was performed) to cross validate the GLM analysis. Then statistical GLM unthresholded spatial maps were compared with the ICs unthresholded, Gaussianized spatial maps by using simple Pearson correlation as measure of "spatial similarity" (Smith et al., 2009). Finally the RSNs depicted by the functionally similar ICs are described briefly according to the terminology used by Beckmann et al. (2005), Damoiseaux et al. (2006) and De Luca et al. (2006).

Subject	Microstate	Corresponding BOLD IC	Functional similarity	Spatial similarity	BOLD IC depicted resting-state network
A	4	3	9.29	0.34	Sensory motor system
	7	6	8.64	0.53	Default mode network
	10	15	6.55	0.23	Executive functions
B	1	10	5.84	0.42	Lateral visual cortical areas
	4	5	24.66	0.55	Auditory system
	5	5	28.17	0.64	Auditory system
	7	5	9.67	0.50	Auditory system
	8	5	9.8	0.33	Auditory system
	9	24	5.54	0.15	Dorsal pathway
C	1	27	10.1	0.19	Dorsal pathway
	2	27	9.98	0.33	Dorsal pathway
	3	5	22.41	0.45	Default mode network
	4	9	16.75	0.43	Default mode network
	5	9	5.58	0.42	Default mode network
	6	16	8.84	0.40	Right dorsal pathway
	7	27	6.09	0.16	Dorsal pathway
	9	5	8.67	0.22	Default mode network
D	2	16	9.41	0.28	Visuospatial and executive system
	4	9	6.83	0.33	Ventral pathway
	5	4	6.41	0.09	Default mode network
	7	5	6.67	0.20	Left dorsal pathway
	8	17	3.22	0.26	Right dorsal pathway
	10	3	9.6	0.47	Sensory motor system
E	5	17	8.43	0.21	Ventral pathway
	6	27	6.68	0.34	Auditory system
	8	30	8.7	0.54	Executive functions
F	2	14	4.73	0.31	Dorsal pathway
	4	6	7.97	0.38	Dorsal central pathway
	5	7	4.31	0.49	Medial visual cortical areas
	9	14	4.39	0.35	Dorsal pathway
	10	26	3.79	0.11	Dorsal pathway/executive functions
G	2	26	4.22	0.34	Dorsal pathway
	3	13	16.13	0.66	Sensory motor system
	4	24	4.37	0.4	Default mode network
	7	24	5.68	0.42	Default mode network
	8	13	19.59	0.7	Sensory motor system
	9	13	8.53	0.55	Sensory motor system
H	1	18	3.33	0.04	Dorsal pathway
	4	16	5.54	0.29	Dorsal pathway
	8	25	3.55	0.05	Sensory motor system
	9	11	8.49	0.41	Medial visual cortical areas
I	2	6	8.61	0.29	Lateral visual cortical areas
	4	24	7.96	0.21	Left dorsal pathway
	9	19	8.01	0.21	Right ventral pathway
J	3	20	6.58	0.21	Dorsal pathway
	5	30	16.18	0.23	Right posterior dorsal pathway
	6	20	29.05	0.33	Dorsal pathway
	7	36	6.9	0.32	Dorsal pathway
	9	28	9.9	0.23	Default mode network
	10	39	21.38	0.23	Ventral pathway
K	1	9	6.95	0.27	Medial visual cortical areas
	2	9	4.05	0.14	Medial visual cortical areas
	5	9	9.11	0.32	Medial visual cortical areas
	7	11	3.18	0.12	Cerebellum frontal cortex
	9	16	5.71	0.18	Visuospatial and executive system

dent factor (Fig. 3), only the *4th factor* was able to elicit BOLD activation surviving the cluster significance threshold of $Z>2.0$. Fig. 6 displays a fronto-occipital network, which includes bilateral subcallosal cortex, bilateral frontal medial cortex, left frontal pole, bilateral paracingulate gyrus, left precentral gyrus, right posterior cingulate cortex, right temporal occipital fusiform cortex, bilateral occipital fusiform gyrus, bilateral lingual gyrus, right parahippocampal gyrus and right precuneus cortex (for detailed information see Table 4). The most consistent part of this network is distributed in the occipital cortex and overlaps substantially with the primary and secondary visual RSNs described by Beckmann and Smith (2004) and Beckmann et al. (2005), while in its prefrontal cortex and posterior cingulated components it shows a substantial overlap to the *default mode network* as described by Raichle et al. (2001) and Greicius et al. (2003). The CSD map of this factor shows also a correspondence with the EEG informed higher level fMRI, displaying an equivalent fronto-occipital network.

To assess the extent to which this network is consistent with well known RSNs we performed a "multi-session temporal concatenation PICA," a data-driven and EEG independent fMRI approach. We found that at group level the PICA decomposition generated 39 ICs spatial maps and related time courses. The activation pattern elicited by the 4th factor microstate-modulated group level GLM analysis is partially "captured" in BOLD ICs showing a high score in the Pearson *r*

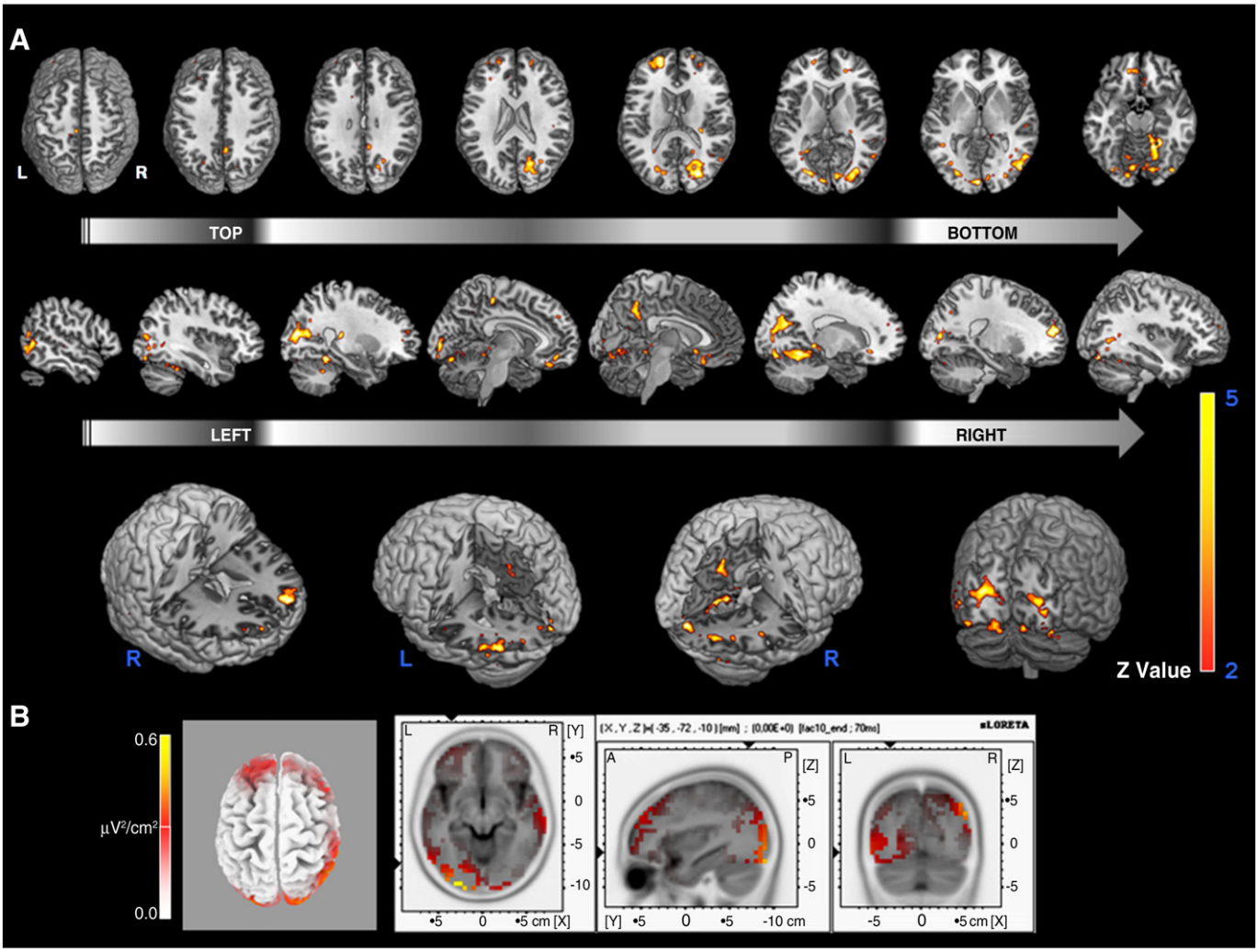

Fig. 6. EEG informed resting fMRI group analysis. A. Group level mixed effect analysis: the design matrix included all microstates across the 11 subjects, each weighted according to the *4th microstate aggregation factor*, BOLD activation was present (cluster significance threshold of $Z>2.0$) in a fronto-occipital network (for detailed information see Table 4). The first row shows axial slices in dorso-ventral direction, and all images have been coregistered into the space of the MNI template. Cluster-corrected threshold $Z=2$, $p=0.05$, L = left, R = right. The second row shows sagittal slices in direction left–right, and all images have been coregistered into the space of the MNI template. Cluster-corrected threshold $Z=2$, $p=0.05$. The third row displays the before mentioned fronto-occipital network Z-map onto a 3D MNI brain model. Corrected threshold $Z=2$, $p=0.05$, L = left, R = right. B. sLORETA CSD maps (μV2/cm^2) show the averaged electrophysiological landscape correspondent to the *4th microstate aggregation factor*. On the left a CSD map projected onto a 3D Talairach model of the brain, while on the right the same CSD map in axial, sagittal and coronal views. The CSD map of this factor shows also a correspondence with the EEG informed higher level fMRI, displaying an equivalent fronto-occipital network.

correlation coefficient as expression of "spatial similarity." Results are shown in Fig. 7. Here we gathered the five PICA-estimated group resting patterns which scored higher on their spatial similarity (Pearson ρ) to the 4th microstate aggregation factor group level statistical spatial map. ICs are classified according to MELODIC (IC number) and all depict functionally relevant RSNs.

IC 37 shows a pattern identifying the *medial visual cortical areas*. These include primary visual areas located in the calcarine sulcus bilaterally as well as medial, but not lateral, extrastriate regions such as the lingual gyrus.

IC 39 consists predominantly of the peristriate area, and lateral and superior occipital gyrus, which are areas recognized as part of the visual cortex.

IC 17 shows a pattern identifying the *executive control* areas. These include superior and middle prefrontal cortices, anterior cingulate and paracingulate gyri, and ventrolateral prefrontal cortex.

IC 13 consists predominantly of the *lateral visual cortical areas*. These included the occipital pole extending laterally towards the occipito-temporal junction, encompassing nonprimary regions of visual cortex.

IC 8 covers the posterior parietal cortex at the occipitoparietal junction, along the midline in the precuneus and posterior cingulate cortex, and in the frontal pole and resembles the already described *default mode network*.

Discussion

The present work was inspired by several experimental studies in the electrophysiology field which, starting from the pioneering work of Lehmann, gave rise to a novel way to look at the EEG signal (Brandeis and Lehmann, 1989; Fingelkurts, 2004; Lehmann and Skrandies, 1980; Lehmann et al., 1987; Lehmann et al., 1998; Michel et al., 2004; Pascual-Marqui et al., 1995; Wackermann et al., 1993; Zhou et al., 1999). Being uniquely characterized by a fixed spatial distribution of active neuronal generators with time varying intensity, a brain microstate might be considered as an electrophysiological fingerprint of specific neural processes occurring during relaxed wakefulness, such as mental imagery, abstract thought, sensory perception or memory retrieval (Lehmann et al., 1998, 2004, 2006; Koenig et al., 1998). When analyzing our multimodal imaging datasets

Table 4
Brain regions in which the EEG-segment regressors weighted according to the 4th microstate aggregation factor showed a positively correlated BOLD signal. Altogether 18,279 voxels were actively divided in 2 clusters (with local maxima).

Anatomical region[a]	MNI coordinates[b] (*X*, *Y*, *Z*)	*Z* value	Cluster index
Right cerebellum, anterior lobe, culmen; Right temporal occipital fusiform cortex[c]	42, −44, −28	4.48	2
Left cerebellum, posterior lobe, declive; Left occipital fusiform gyrus[c] [BA19]	−32, −84, −18	4.23	2
Right lateral occipital cortex [BA7, 17[c]]	26, −82, 12	4.14	2
Right precuneus cortex [BA18]	18, −52, 14	4.12	2
Right cerebellum, anterior lobe; right temporal occipital fusiform cortex[c]	24, −48, −16	4.01	2
Left occipital pole [BA17]	−4, −92, 0	3.99	2
Right cingulate gyrus posterior division [BA31]	6, −54, 36	3,75	2
Left frontal pole [BA10]	−20, 58, 16	3.93	1
Left frontal pole [BA11]	−20, 52, 12	3.85	1
Right frontal pole [BA9]	18, 50, 20	3.52	1
Left frontal pole [BA10]	−30, 54, 18	3.5	1
Right frontal pole [BA10]	20, 62, 16	3.46	1
Left frontal medial cortex [BA11, 10[c], 32[c]]	−14, 42, −16	3.4	1

[a] According to the Harvard–Oxford structural atlas.
[b] Local maxima.
[c] Activation extended also to this area (Talairach daemon labels).

from the perspective of the 'EEG microstate segmentation' we are guided by a direct measure of neuronal activity rich in information in the spatial (microstate as punctual source distribution), temporal (microstate as recurrent electrophysiological landscape in specific time epochs) and spectral domain (microstate as carrier of a specific coalescence of rhythms). We expected that this richness in EEG information might be complemented by the high spatial resolution afforded by fMRI in order to detect more precisely cortical neuronal generators. Moreover, since in the fMRI field RSNs are now well described we wanted to verify whether those networks are related to the EEG microstates.

Using the EEG microstates to model the HRF, we observed that half of the microstates (pro subject mean: 5 ± 1.6 SD) were able to elicit BOLD activation at the single subject level in all the investigated volunteers (Table 3, Supplementary Table 1 and Supplementary Fig. 1a–j). The BOLD patterns elicited are consistent with well known RSNs such as the default mode network, the dorsal and ventral pathways (bilateral as well as lateralized), the sensory motor system, the auditory system, the executive function system, the lateral and medial visual cortical areas, the visuospatial and executive system (Biswal et al., 1995; Rivier and Clarke, 1997; Raichle et al., 2001; Greicius et al., 2003; Beckmann and Smith, 2004; Beckmann et al., 2005; Damoiseaux et al., 2006; De Luca et al., 2006). Furthermore our results are corroborated by the BOLD PICA replicating the findings from Beckmann et al. (2005) about consistent RSNs across subjects. The PICA decomposition revealed several "native BOLD ICs" which were not only functionally similar to the microstate regressors, i.e. temporally correlated (high *F* value), but also spatially similar (high *r* value) to the microstate elicited BOLD activation. Some of the abovementioned RSNs clusters are depicted as selected examples in Fig. 5, while all results are summarized in Table 3 (a visual overview is available in Supplementary Fig. 1a–j). Here EEG microstates, which elicited BOLD activation (classified according to sLORETA), are reported alongside ICs (PICA decomposition) selected on the basis of their functional similarity (the ICs which scored higher on *F* value); the spatial similarity (simple Pearson correlation) is also reported. Our results show that it is possible to model spontaneous fluctuations in BOLD signal by using EEG microstate parameters in the GLM. By utilizing the excellent temporal resolution of spontaneous fluctuations in EEG activity to guide our analysis of the fMRI data we have shown BOLD activation in known RSNs that is associated with these microstates. So while most previous fMRI research on RSNs has relied on predominantly indirect measures of neural activity our approach is guided by a neuronal native signal, demonstrating for the first time

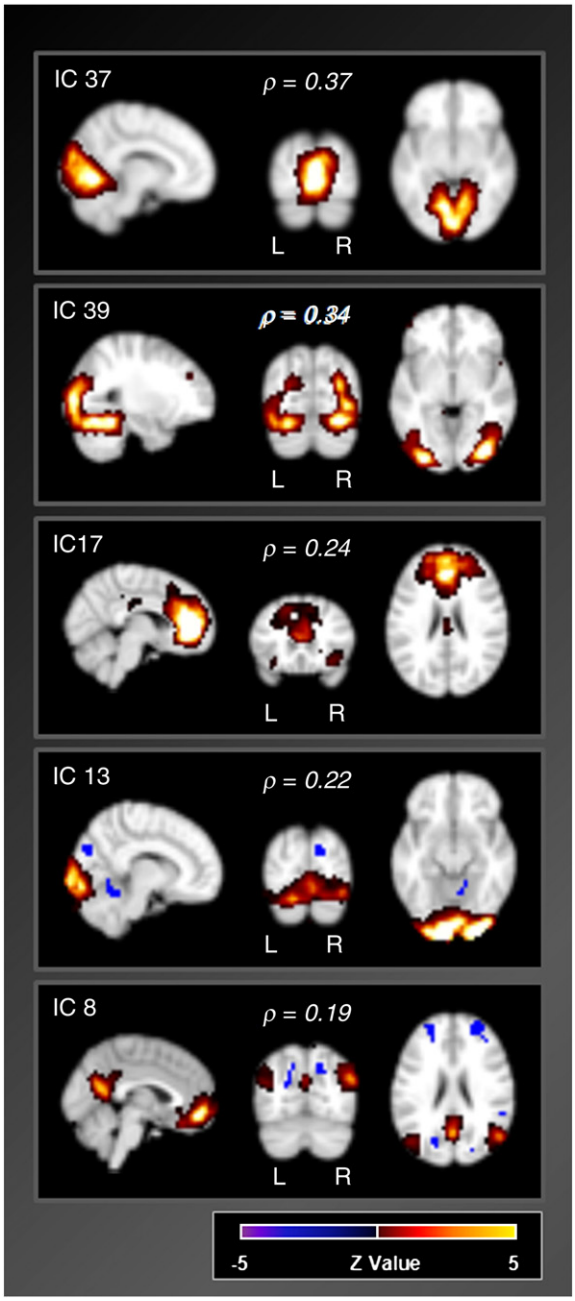

Fig. 7. Cross validating resting fMRI group ICA analysis. Five PICA-estimated resting patterns: Sagittal, coronal and axial views of different spatial maps associated with low-frequency resting patterns estimated from a group of 11 subjects. All images have been coregistered into the space of the MNI template. The group BOLD ICs are classified according to MELODIC (IC number on the top left) and ordered according to their "spatial similarity" (Pearson ρ) to the 4th microstate aggregation factor group level statistical spatial map. Images are shown in neurological convention, cluster-corrected threshold $Z=2$, $p=0.05$ (an additional $Z=-2$, $p=0.05$ statistical map is superimposed to also show the negative correlation when present), L = left, R = right. IC 37 shows a pattern identifying the *medial visual cortical areas*. IC 39 consists predominantly of the peristriate area, and lateral and superior occipital gyrus, which are areas recognized as part of the visual cortex. IC 17 shows a pattern identifying the *executive control* areas. IC 13 consists predominantly of the *lateral visual cortical areas*. IC 8 resembles the already described *default mode network*.

that those BOLD RSNs are related to the synchronous firing of neuronal assemblies.

Nonetheless, at the single subject level the microstate-modulated fMRI regressors showed a large variability with regard to the BOLD signal patterns emerging from this specific analysis approach. The 55 elicited activation patterns are characterized by remarkable differences among clusters dimensions varying from 10,101 down to 46 voxels (Supplementary Table 1), so that the temporal correlation to BOLD ICs alone would not be sufficient for a cross validation. In fact PICA proved useful as a cross validation method only when both the functional and the spatial similarity criteria were fulfilled. Indeed these two criteria are linked showing a significant positive linear relationship ($r = 0.48$, $p < 0.0002$, two tailed).

Another aspect of this variability is that among ten identified microstates only three were temporally significantly correlated to variations in the BOLD signal intensity in certain subjects while in other subjects up to eight microstates elicited significant activation. The mean percentage of total EEG duration in each microstate was 5%. Interestingly only microstates which represent a 5% to 25% of the absolute length of the EEG (due to their occurrence rate and duration) were significantly correlated to spontaneous fluctuation of BOLD signal. Microstates under the 5%, i.e., showing up rarely or for a short time-window, were apparently not stable and strong enough to go along with an increase in the metabolic demand of the involved brain areas. On the other hand, microstates above 25% of the total EEG duration are accompanied by the problem of "fast event related design" leading to BOLD saturation and hence have low power (Henson et al., 2002). Nevertheless, the number of ten microstates was revealed to be optimal to catch the spontaneous fluctuation of BOLD signal in EEG modeled GLM analysis, since more than ten would lead to sparse landscape occurrence and or short duration, while less than ten microstates would lead to dense landscape occurrence and/or long duration both with an impact on the statistical power.

A major issue in conducting a group fMRI analysis using the EEG microstate informed single subject contrast of parameter estimates (COPEs) is in fact the intrinsic high inter-subject variability of the microstates distribution present during brain spontaneous activity. This variability is also reflected by the fact that sLORETA provides a heterogeneous classification: what is defined "microstate 1" in "subject A" does not necessarily correspond (in its landscape) to the same microstate number in "subject B" so that a factor analysis across subjects was necessary. Using the output of the factor analysis as a "compass" to get oriented across the "landscapes," we were able to run a group fMRI analysis. Of the 7 aggregation factors identified, only the 4th factor survived the cluster threshold (Z-score ≥ 2.0). This might be explained by the fact that the group mixed effect fMRI analysis fails to detect non-uniform brain activity which is the case in a sample with a high inter-subject variability. This is especially true in a resting-state condition in which different neural processes follow one another or are superimposed while a control condition or a behavioral output is missing. In other words, even if EEG microstates at the single subject level proved to be a sort of fingerprint of the ongoing activity and are also correlated positively with BOLD signal changes, at the group level their heterogeneity leads to a lack of statistical power so that their richness in information is lost in the averaging process. Nevertheless, as displayed in Fig. 6 the 4th factor, which might be described as a fronto-occipital network, survived the threshold. To search for similarities between this network and already acknowledged RSNs, we performed a "multi-session temporal concatenation PICA," as cross validation at the group level. We found that the PICA decomposition generated 39 ICs spatial maps and related time courses. The activation pattern elicited by the 4th factor microstate-modulated group level GLM analysis overlaps sensibly to several "native BOLD group ICs" showing a high score in spatial similarity. Fig. 7 depicts the five PICA-estimated group resting patterns which scored higher (Pearson ρ) and all show functionally relevant RSNs located mainly in the occipital (IC 37: *medial visual cortical areas*; IC 39 and IC 13: *lateral visual cortical areas*) and frontal areas (IC 17: *executive control* areas) as well as the well known *default mode network* (IC 8).

Concerning the correspondence between the EEG CSD maps and fMRI activation patterns, we have to conclude that our setup is not sufficiently sophisticated for this purpose. Indeed simulation and experimental studies suggest that at least 60 (but preferably more) equally distributed electrodes are required for accurate spatial sampling of scalp activities i.e. EEG source localization and that it is recommended to digitize the electrodes positions (Lantz et al., 2003; Luu et al., 2001). Although intriguing, a quantitative assessment of the EEG sources and their correspondence with the fMRI activation maps is thus beyond the scope of this paper, so that our CSD maps are only for displaying purposes. Such analysis approach would require the same solution space for EEG and fMRI analysis and the same decomposition strategy for both the electrical and magnetic resonance signal in the so-called "EEG/fMRI fusion analysis approach" (Laufs et al., 2008). Finally, we have to consider that the correspondence between microstates and resting BOLD fluctuation goes in both directions with microstates being functionally related to more than one BOLD ICs and vice versa BOLD ICs functionally related to more microstates with different degrees of spatial similarity with respect to the elicited EEG-modulated BOLD activation maps. Thus, whether microstates represent the origin or consequence of BOLD resting fluctuation deserves further investigations, showing our data once more how electrophysiological, metabolic and vascular events in the brain are not identical and probably only partially overlapped.

To our knowledge, this is the first work which successfully used the microstate information to guide an fMRI analysis in a multimodal imaging setting. Integration of the electrophysiological and hemodynamic data in this way allows to maximize the temporal and spatial aspects of our data, thus providing a framework for further comprehensive multi-model investigation of the brain at rest.

Acknowledgments

This work was supported by an internal grant of the Heinrich-Heine University Duesseldorf.

We thank Daria Orzechowski, Anja Müller-Reinhartz and Birgitta Sasse for technical assistance.

Appendix A. Supplementary data

Supplementary data associated with this article can be found, in the online version, at doi:10.1016/j.neuroimage.2010.01.093.

References

Allen, P., Josephs, O., Turner, R., 2000. A method for removing imaging artifact from continuous EEG recorded during functional MRI. NeuroImage 1, 230–239.

Allen, P., Polizz, G., Krakow, K., Fish, D.R., Lemieux, L., 1998. Identification of EEG events in the MR scanner: the problem of pulse artifact and a method for its subtraction. NeuroImage 8, 229–239.

Arieli, A., Sterkin, A., Grinvald, A., Aertsen, A., 1996. Dynamics of ongoing activity: explanation of the large variability in evoked cortical responses. Science 27 (273), 1868–1871.

Beckmann, C.F., Smith, S.M., 2004. Probabilistic independent component analysis for functional magnetic resonance imaging. IEEE Trans. Med. Imag. 23 (2), 137–152.

Beckmann, C.F., Smith, S.M., 2005. Tensorial extensions of independent component analysis for multisubject FMRI analysis. NeuroImage 25, 294–311.

Beckmann, C.F., Noble, J.A., Smith, S.M., 2001. Investigating the intrinsic dimensionality of FMRI data for ICA. NeuroImage 13, S76.

Beckmann, C.F., DeLuca, M., Devlin, J.T., Smith, S.M., 2005. Investigations into resting-state connectivity using independent component analysis. Philos. Trans. R Soc. Lond. B Biol. Sci. 360 (1457), 1001–1013.

Behrens, T., Woolrich, M.W., Smith, S., 2003. Multi-testing Using a Fully Subject Null Hypothesis Bayesian Framework: Theory. Human Brain Mapping Meeting, New York City.

Berger, H., 1929. Über das Elektrenkephalogramm des Menschen. Arch. Psychiatr. Nervenkr. 87, 527–570.

Brandeis, D., Lehmann, D., 1989. Segments of ERP map series reveal landscape changes with visual attention and subjective contours. Electroencephalogr. Clin. Neurophysiol. 73, 507–519.
Biswal, B., Yetkin, F., Haughton, V., Hyde, J., 1995. Functional connectivity in the motor cortex of resting human brain using echo-planar MRI. Magn. Res. Med. 34, 537–541.
Cordes, D., et al., 2001. Frequencies contributing to functional connectivity in the cerebral cortex in 'resting-state' data. Am. J. Neuroradiol. 22, 1326–1333.
Damoiseaux, J.S., Rombouts, S.A.R.B., Barkhof, F., Scheltens, P., Stam, C.J., Smith, S.M., Beckmann, C.F., 2006. Consistent resting-state networks across healthy subjects. Proc. Natl. Acad. Sci. U. S. A. 103, 13848–13853.
De Luca, M., Beckmann, C.F., De Stefano, N., Matthews, P.M., Smith, S.M., 2006. fMRI resting state networks define distinct modes of long-distance interactions in the human brain. NeuroImage 29, 1359–1367.
De Munck, J., Gonçalves, S.I., Huijboom, L., Kuijer, J.P.A., Pouwels, P.J.W., Heethaar, R.M., Lopes da Silva, F.H., 2007. The hemodynamic response of the alpha rhythm: an EEG/fMRI study. NeuroImage 35, 1142–1151.
Fingelkurts, A.A., 2004. Making complexity simpler: multivariability and metastability in the brain. Int. J. Neurosci. 114, 843–862.
Forman, S.D., Cohen, J.D., Fitzgerald, M., Eddy, W.F., Mintun, M.A., Noll, D.C., 1995. Improved assessment of significant activation in functional magnetic resonance imaging (fMRI): use of a cluster-size threshold. Magn. Reson. Med. 33, 636–647.
Fox, M.D., Raichle, M.E., 2007. Spontaneous fluctuations in brain activity observed with functional magnetic resonance imaging. Nature 8 (700), 700–711.
Fox, M.D., Snyder, A.Z., Zacks, J.M., Raichle, M.E., 2006. Coherent spontaneous activity accounts for trial-to trial variability in human evoked brain responses. Nat. Neurosci. 9, 23–25.
Fransson, P., 2005. Spontaneous low-frequency BOLD signal fluctuations: an fMRI investigation of the resting-state default mode of brain function hypothesis. Hum. Brain Mapp 26, 15–29.
Friston, K.J., Williams, S., Howard, R., Frackowiak, R.S., Turner, R., 1996. Movement-related effects in fMRI time-series. Magn. Reson. Med. 35 (3), 346–355.
Fuchs, M., Kastner, J., Wagner, M., Hawes, S, Ebersole, J.S., 2002. A standardized boundary element method volume conductor model. Clin. Neurophysiol. 113, 702–712.
Goldman, R.I., Stern, J.M., Engel, J., Cohen, M.S., 2002. Tomographic mapping simultaneous EEG/fMRI of the alpha rhythm. Neuroreport 13 (18), 2487–2492 Dec 20.
Greicius, M.D., Krasnow, B., Reiss, A.L., Menon, V., 2003. Functional connectivity in the resting brain: a network analysis of the default mode hypothesis. Proc. Natl. Acad. Sci. U. S. A. 100, 253–258.
Hyvärinen, A., 1999. Fast and robust fixed-point algorithms for independent component analysis. IEEE Trans. Neural Netw. 10 (3), 626–634.
Henson, R.N., Price, C.J., Rugg, M.D., Turner, R., Friston, K.J., 2002. Detecting latency differences in event-related BOLD responses: application to words versus non-words and initial versus repeated face presentations. Neuroimage 15, 83–97.
Holmes, A.P., Blair, R.C., Watson, J.D., Ford, I., 1996. Nonparametric analysis of statistical images from functional mapping experiments. J. Cereb. Blood Flow Metab. 16, 7–12.
Ives, J.R., Warach, S., Schmitt, F., Edelman, R.R., Schomer, D.L., 1993. Monitoring the patient's EEG during echo planar MRI. Electroencephalogr. Clin. Neurophysiol. 87 (6), 417–420.
Jenkinson, M., Bannister, P., Brady, J., Smith, S., 2002. Improved optimization for the robust and accurate linear registration and motion correction of brain images. NeuroImage 17, 825–841.
Jurcak, V., Tsuzuki, D., Dan, I., 2007. 10/20, 10/10, and 10/5 systems revisited: their validity as relative head-surface-based positioning systems. NeuroImage 34, 1600–1611.
Koenig, T., Kochi, K., Lehmann, D., 1998. Event-related electric microstates of the brain differ between words with visual and abstract meaning. Electroencephalogr. Clin. Neurophysiol. 106, 535–546.
Lancaster, J.L., Woldorff, M.G., Parsons, L.M., Liotti, M., Freitas, C.S., Rainey, L., Kochunov, P.V., Nickerson, D., Mikiten, S.A., Fox, P.T., 2000. Automated Talairach atlas labels for functional brain mapping. Hum. Brain Mapp. 10, 120–131.
Lantz, G., Grave, d. P., Spinelli, L., Seeck, M., Michel, C.M., 2003. Epileptic source localization with high density EEG: how many electrodes are needed? Clin. Neurophysiol. 114, 63–69.
Laufs, H., 2008. Endogenous brain oscillations and related networks detected by surface EEG-combined fMRI. Hum. Brain Mapp. 29, 762–769.
Laufs, H., Kleinschmidt, A., Beyerle, A., Eger, E., Salek-Haddadi, A., Preibisch, C., Krakow, K., 2003a. EEG-correlated fMRI of human α activity. Neuroimage 19, 1463–1476.
Laufs, H., Krakow, K., Sterzer, P., Eger, E., Beyerle, A., Salek-Haddadi, A., Kleinschmidt, A., 2003b. Electroencephalographic signatures of attentional and cognitive default modes in spontaneous brain activity fluctuations at rest. Proc. Natl. Acad. Sci. U. S. A. 100, 11053–11058.
Laufs, H., Holt, J.L., Elfont, R., Krams, M., Paul, J.S., Krakow, K., Kleinschmidt, A., 2006. Where the BOLD signal goes when a EEG leaves. Neuroimage 31, 1408–1418.
Laufs, H., Daunizeau, J., Carmichael, D.W., Kleinschmidt, A., 2008. Recent advances in recording electrophysiological data simultaneously with magnetic resonance imaging. NeuroImage 40 (2), 515–528.
Lehmann, D., 1971. Multichannel topography of human alpha EEG fields. Electroencephalogr. Clin. Neurophysiol. 31, 439–449.
Lehmann, D., 1987. Principles of spatial analysis. In: Gevins, A., Remond, A. (Eds.), Handbook of Electroencephalography and Clinical Neurophysiology, Methods of Analysis of Brain Electrical and Magnetic Signals, Vol. 1. Elsevier, Amsterdam, pp. 309–354.
Lehmann, D., Skrandies, W., 1980. Reference-free identification of components of checkerboard-evoked multichannel potential fields. Electroencephalogr. Clin. Neurophysiol. 48, 609–621.
Lehmann, D., Ozaki, H., Pal, I., 1987. EEG alpha map series: brain micro-states by space-oriented adaptive segmentation. Electroencephalogr. Clin. Neurophysiol. 67, 271–288.
Lehmann, D., Strik, W.K., Henggeler, B., Koenig, T., Koukkou, M., 1998. Brain electric microstates and momentary conscious mind states as building blocks of spontaneous thinking: I. Visual imagery and abstract thoughts. Int. J. Psychophysiol. 29, 1–11.
Lehmann, D., Koenig, T., Henggeler, B., Strik, W., Kochi, K., Koukkou, M., Pascual-Marqui, R.D., 2004. Brain areas activated during electric microstates of mental imagery versus abstract thinking. Klin. Neurophysiol. 35, 169.
Lehmann, D., Faber, P.L., Gianotti, L.R., Kochi, K., Pascual-Marqui, R.D., 2006. Coherence and phase locking in the scalp EEG and between LORETA model sources, and microstates as putative mechanisms of brain temporo-spatial functional organization. J. Physiol. - Paris 99, 29–36.
Lowe, M.J., Mock, B.J., Sorenson, J.A., 1998. Functional connectivity in single and multislice echoplanar imaging using resting-state fluctuations. Neuroimage 7, 119–132.
Luu, P., Tucker, D.M., Englander, R., Lockfeld, A., Lutsep, H., Oken, B., 2001. Localizing acute stroke-related EEG changes: assessing the effects of spatial undersampling. J. Clin. Neurophysiol. 18, 302–317.
Mantini, D., Perrucci, M.G., Del Gratta, C., Romani, G.L., Corbetta, M., 2007. Electrophysiological signatures of resting state networks in the human brain. Proc. Natl. Acad. Sci. U. S. A. 104, 13170–13175.
Mazziotta, J., Toga, A., Evans, A., Fox, P., Lancaster, J., Zilles, K., Woods, R., Paus, T., Simpson, G., Pike, B., Holmes, C., Collins, L., Thompson, P., MacDonald, D., Iacoboni, M., Schormann, T., Amunts, K., Palomero-Gallagher, N., Geyer, S., Parsons, L., Narr, K., Kabani, N., Le Goualher, G., Boomsma, D., Cannon, T., Kawashima, R., and Mazoyer, B. 2001. A probabilistic atlas and reference system for the human brain: International Consortium for Brain Mapping (ICBM). Philos. Trans. R Soc. Lond. B Biol. Sci. 29, 356(1412), 1293-1322.
Michel, C.M., Murray, M.M., Lantz, G., Gonzalez, S., Spinelli, L., Grave de Peralta, R., 2004. EEG source imaging. Clin. Neurophysiol. 115, 2195–2222.
Minka, T. 2000. Automatic choice of dimensionality for PCA. Technical Report 514, MIT Media Lab Vision and Modeling Group.
Moosmann, M., et al., 2003. Correlates of α rhythm in functional magnetic resonance imaging and near infrared spectroscopy. Neuroimage 20, 145–158.
Oostenveld, R., Praamstra, P., 2001. The five percent electrode system for high-resolution EEG and ERP measurement. Clin. Neurophysiol. 112, 713–719.
Pascual-Marqui, 2002. Standardized low-resolution brain electromagnetic tomography (sLORETA): technical details. Methods Find Exp. Clin. Pharmacol. 24 (Suppl. D), 5–12.
Pascual-Marqui, R.D., 1999. Review of methods for solving the EEG inverse problem. Int. J. Bioelectromagn. 1, 75–86.
Pascual-Marqui, R.D., Michel, C.M., Lehmann, D., 1994. Low resolution electromagnetic tomography: a new method for localizing electrical activity in the brain. Int. J. Psychophysiol. 18, 49–65.
Pascual-Marqui, R.D., Michel, C.M., Lehmann, D., 1995. Segmentation of brain electrical activity into microstates: model estimation and validation. IEEE Trans. Biomed. Eng. 42 (7), 658–665.
Rademacher, J., Morosan, P., Schormann, T., Schleicher, A., Werner, C., Freund, H.-J., Zilles, K., 2001. Probabilistic mapping and volume measurement of human primary auditory cortex. NeuroImage 13, 669–683.
Raichle, M.E., Mintun, M.A., 2006. Brain work and brain imaging. Annu. Rev. Neurosci. 29, 449–476.
Raichle, M.E., Snyder, A.Z., 2007. A default mode of brain function: a brief history of an evolving idea. Neuroimage 37, 1083–1090.
Raichle, M.E., MacLeod, A.M., Snyder, A.Z., Powers, W.J., Gusnard, D.A., Shulman, G.L., 2001. A default mode of brain function. Proc. Natl. Acad. Sci. U. S. A. 98, 676–682.
Rivier, F., Clarke, S., 1997. Cytochrome oxidase, acetylcholinesterase, and nadph-diaphorase staining in human supratemporal and insular cortex: evidence for multiple auditory areas. NeuroImage 6, 288–304.
Rorden, C., Karnath, H.O., Bonilha, L., 2007. Improving lesion-symptom mapping. J. Cogn. Neurosci. 19, 1081–1088.
Salek-Haddadi, A., Friston, K.J., Lemieux, L., Fish, D.R., 2003. Studying spontaneous EEG activity with fMRI. Brain Res. Rev. 43, 110–113.
Smith, S., 2002. Fast robust automated brain extraction. Hum. Brain Mapp. 17, 143–155.
Smith, S.M., Fox, P.T., Miller, K.L., Glahn, D.C., Fox, P.M., Mackay, C.E., Filippini, N., Watkins, K.E., Toro, R., Laird, A.R., Beckmann, C.F., 2009. Correspondence of the brain's functional architecture during activation and rest. Proc. Natl. Acad. Sci. U. S. A. 106, 13040–13045.
Szava, S., Valdes, P., Biscay, R., Galan, L., Bosch, J., Clark, I., Jimenez, J.C., 1994. High resolution quantitative EEG analysis. Brain Topogr. 6, 211–219.
Tipping, M.E., Bishop, C.M, 1999. Probabilistic principal component analysis. J. R. Stat. Soc. B 61 (3), 611–622.
Tsodyks, M., Kenet, T., Grinvald, A., Arieli, A., 1999. Linking spontaneous activity of single cortical neurons and the underlying functional architecture. Science 3 (286), 1943–1946.
Wackermann, J., Lehmann, D., Michel, C.M., Strik, W.K., 1993. Adaptive segmentation of spontaneous EEG map series into spatially defined microstates. Int. J. Psychophysiol. 14, 269–283.
Warbrick, T., Mobascher, A., Brinkmeyer, J., Musso, F., Richter, N., Stoecker, T., Fink, G.R., Shah, N.J., Winterer, G., 2009. Single-trial P3 amplitude and latency informed event-related fMRI models yield different BOLD response patterns to a target detection task. NeuroImage 47, 1532–1544.
Woolrich, M.W., Ripley, B.D., Brady, M., Smith, S.M., 2001. Temporal autocorrelation in univariate linear modelling of fMRI data.
Worsley, K.J., Evans, A.C., Marrett, S., Neelin, P., 1992. A three-dimensional statistical analysis for CBF activation studies in human brain. J. Cereb. Blood Flow Metab. 12, 900–918.
Zhou, S., Wang, C., Wei, J., Wu, S., 1999. Fuzzy segmentation spatiotemporal patterns of cognitive potential into microstates. Brain Topogr. 12, 61–67.